



Fermi National Accelerator Laboratory

FERMILAB-Conf-96/163-E

D0

**Search for a Fourth Generation Charge – $1/3$ Quark via Flavor
Changing Neutral Currents**

S. Abachi et al.

The D0 Collaboration

*Fermi National Accelerator Laboratory
P.O. Box 500, Batavia, Illinois 60510*

July 1996

Submitted to the *28th International Conference on High Energy Physics (ICHEP96)*,
Warsaw, Poland, July 25-31, 1996

Disclaimer

This report was prepared as an account of work sponsored by an agency of the United States Government. Neither the United States Government nor any agency thereof, nor any of their employees, makes any warranty, expressed or implied, or assumes any legal liability or responsibility for the accuracy, completeness, or usefulness of any information, apparatus, product, or process disclosed, or represents that its use would not infringe privately owned rights. Reference herein to any specific commercial product, process, or service by trade name, trademark, manufacturer, or otherwise, does not necessarily constitute or imply its endorsement, recommendation, or favoring by the United States Government or any agency thereof. The views and opinions of authors expressed herein do not necessarily state or reflect those of the United States Government or any agency thereof.

Search for a Fourth Generation Charge $-1/3$ Quark via Flavor Changing Neutral Currents

The DØ Collaboration¹
(July 1996)

There is some likelihood that a light ($< m_t$) fourth generation charge $-1/3$ quark (b') would decay predominantly via loop induced flavor changing neutral currents. The charged current decay of b' to charm would be highly Cabibbo suppressed due to the fact that it changes the generation number by two. The DØ experiment has searched for b' pair production where one or both b' quarks decays via $b' \rightarrow b + \gamma$, giving signatures photon + three jets and two photons + two jets. We do not see a significant excess of such events over background. In both modes, we set an upper limit on the cross section times branching ratio that is sufficient to rule out a standard sequential b' decaying predominantly via FCNC in the mass range $m_Z/2 < m_{b'} < m_Z + m_b$. For b' masses larger than this, the dominant FCNC decay mode is expected to be $b' \rightarrow b + Z$.

S. Abachi,¹⁴ B. Abbott,²⁸ M. Abolins,²⁵ B.S. Acharya,⁴³ I. Adam,¹² D.L. Adams,³⁷ M. Adams,¹⁷
 S. Ahn,¹⁴ H. Aihara,²² J. Alitti,⁴⁰ G. Álvarez,¹⁸ G.A. Alves,¹⁰ E. Amidi,²⁹ N. Amos,²⁴
 E.W. Anderson,¹⁹ S.H. Aronson,⁴ R. Astur,⁴² R.E. Avery,³¹ M.M. Baarmand,⁴² A. Baden,²³
 V. Balamurali,³² J. Balderston,¹⁶ B. Baldin,¹⁴ S. Banerjee,⁴³ J. Bantly,⁵ J.F. Bartlett,¹⁴
 K. Bazizi,³⁹ J. Bendich,²² S.B. Beri,³⁴ I. Bertram,³⁷ V.A. Bezzubov,³⁵ P.C. Bhat,¹⁴
 V. Bhatnagar,³⁴ M. Bhattacharjee,¹³ A. Bischoff,⁹ N. Biswas,³² G. Blazey,¹⁴ S. Blessing,¹⁵
 P. Bloom,⁷ A. Boehnlein,¹⁴ N.I. Bojko,³⁵ F. Borchering,¹⁴ J. Borders,³⁹ C. Boswell,⁹
 A. Brandt,¹⁴ R. Brock,²⁵ A. Bross,¹⁴ D. Buchholz,³¹ V.S. Burtovoi,³⁵ J.M. Butler,³
 W. Carvalho,¹⁰ D. Casey,³⁹ H. Castilla-Valdez,¹¹ D. Chakraborty,⁴² S.-M. Chang,²⁹
 S.V. Chekulaev,³⁵ L.-P. Chen,²² W. Chen,⁴² S. Choi,⁴¹ S. Chopra,²⁴ B.C. Choudhary,⁹
 J.H. Christenson,¹⁴ M. Chung,¹⁷ D. Claes,⁴² A.R. Clark,²² W.G. Cobau,²³ J. Cochran,⁹
 W.E. Cooper,¹⁴ C. Cretsinger,³⁹ D. Cullen-Vidal,⁵ M.A.C. Cummings,¹⁶ D. Cutts,⁵ O.I. Dahl,²²
 K. De,⁴⁴ M. Demarteau,¹⁴ N. Denisenko,¹⁴ D. Denisov,¹⁴ S.P. Denisov,³⁵ H.T. Diehl,¹⁴
 M. Diesburg,¹⁴ G. Di Loreto,²⁵ R. Dixon,¹⁴ P. Draper,⁴⁴ J. Drinkard,⁸ Y. Ducros,⁴⁰
 S.R. Dugad,⁴³ D. Edmunds,²⁵ J. Ellison,⁹ V.D. Elvira,⁴² R. Engelmann,⁴² S. Eno,²³ G. Eppley,³⁷
 P. Ermolov,²⁶ O.V. Eroshin,³⁵ V.N. Evdokimov,³⁵ S. Fahey,²⁵ T. Fahland,⁵ M. Fatyga,⁴
 M.K. Fatyga,³⁹ J. Featherly,⁴ S. Feher,¹⁴ D. Fein,² T. Ferbel,³⁹ G. Finocchiaro,⁴² H.E. Fisk,¹⁴
 Y. Fisyak,⁷ E. Flattum,²⁵ G.E. Forden,² M. Fortner,³⁰ K.C. Frame,²⁵ P. Franzini,¹² S. Fuess,¹⁴
 E. Gallas,⁴⁴ A.N. Galyaev,³⁵ T.L. Geld,²⁵ R.J. Genik II,²⁵ K. Genser,¹⁴ C.E. Gerber,¹⁴
 B. Gibbard,⁴ V. Glebov,³⁹ S. Glenn,⁷ J.F. Glicenstein,⁴⁰ B. Gobbi,³¹ M. Goforth,¹⁵
 A. Goldschmidt,²² B. Gómez,¹ G. Gomez,²³ P.I. Goncharov,³⁵ J.L. González Solís,¹¹ H. Gordon,⁴
 L.T. Goss,⁴⁵ N. Graf,⁴ P.D. Grannis,⁴² D.R. Green,¹⁴ J. Green,³⁰ H. Greenlee,¹⁴ G. Griffin,⁸
 N. Grossman,¹⁴ P. Grudberg,²² S. Grünendahl,³⁹ W.X. Gu,^{14,*} G. Guglielmo,³³ J.A. Guida,²
 J.M. Guida,⁵ W. Guryn,⁴ S.N. Gurzhiev,³⁵ P. Gutierrez,³³ Y.E. Gutnikov,³⁵ N.J. Hadley,²³
 H. Haggerty,¹⁴ S. Hagopian,¹⁵ V. Hagopian,¹⁵ K.S. Hahn,³⁹ R.E. Hall,⁸ S. Hansen,¹⁴
 R. Hatcher,²⁵ J.M. Hauptman,¹⁹ D. Hedin,³⁰ A.P. Heinson,⁹ U. Heintz,¹⁴

¹Submitted to the 28th International Conference on High Energy Physics, Warsaw, Poland, 25-31 July 1996.

R. Hernández-Montoya,¹¹ T. Heuring,¹⁵ R. Hirosky,¹⁵ J.D. Hobbs,¹⁴ B. Hoeneisen,^{1,†}
 J.S. Hoftun,⁵ F. Hsieh,²⁴ Tao Hu,^{14,*} Ting Hu,⁴² Tong Hu,¹⁸ T. Huehn,⁹ S. Igarashi,¹⁴ A.S. Ito,¹⁴
 E. James,² J. Jaques,³² S.A. Jerger,²⁵ J.Z.-Y. Jiang,⁴² T. Joffe-Minor,³¹ H. Johari,²⁹ K. Johns,²
 M. Johnson,¹⁴ H. Johnstad,²⁹ A. Jonckheere,¹⁴ M. Jones,¹⁶ H. Jöstlein,¹⁴ S.Y. Jun,³¹
 C.K. Jung,⁴² S. Kahn,⁴ G. Kalbfleisch,³³ J.S. Kang,²⁰ R. Kehoe,³² M.L. Kelly,³² L. Kerth,²²
 C.L. Kim,²⁰ S.K. Kim,⁴¹ A. Klatchko,¹⁵ B. Klima,¹⁴ B.I. Klochkov,³⁵ C. Klopfenstein,⁷
 V.I. Klyukhin,³⁵ V.I. Kochetkov,³⁵ J.M. Kohli,³⁴ D. Koltick,³⁶ A.V. Kostritskiy,³⁵ J. Kotcher,⁴
 J. Kourlas,²⁸ A.V. Kozelov,³⁵ E.A. Kozlovski,³⁵ M.R. Krishnaswamy,⁴³ S. Krzywdzinski,¹⁴
 S. Kunori,²³ S. Lami,⁴² G. Landsberg,¹⁴ J-F. Lebrat,⁴⁰ A. Leflat,²⁶ H. Li,⁴² J. Li,⁴⁴ Y.K. Li,³¹
 Q.Z. Li-Demarteau,¹⁴ J.G.R. Lima,³⁸ D. Lincoln,²⁴ S.L. Linn,¹⁵ J. Linnemann,²⁵ R. Lipton,¹⁴
 Y.C. Liu,³¹ F. Lobkowicz,³⁹ S.C. Loken,²² S. Lökös,⁴² L. Lueking,¹⁴ A.L. Lyon,²³
 A.K.A. Maciel,¹⁰ R.J. Madaras,²² R. Madden,¹⁵ L. Magaña-Mendoza,¹¹ S. Mani,⁷ H.S. Mao,^{14,*}
 R. Markeloff,³⁰ L. Markosky,² T. Marshall,¹⁸ M.I. Martin,¹⁴ B. May,³¹ A.A. Mayorov,³⁵
 R. McCarthy,⁴² T. McKibben,¹⁷ J. McKinley,²⁵ T. McMahon,³³ H.L. Melanson,¹⁴
 J.R.T. de Mello Neto,³⁸ K.W. Merritt,¹⁴ H. Miettinen,³⁷ A. Mincer,²⁸ J.M. de Miranda,¹⁰
 C.S. Mishra,¹⁴ N. Mokhov,¹⁴ N.K. Mondal,⁴³ H.E. Montgomery,¹⁴ P. Mooney,¹ H. da Motta,¹⁰
 M. Mudan,²⁸ C. Murphy,¹⁷ F. Nang,⁵ M. Narain,¹⁴ V.S. Narasimham,⁴³ A. Narayanan,²
 H.A. Neal,²⁴ J.P. Negret,¹ E. Neis,²⁴ P. Nemethy,²⁸ D. Nešić,⁵ M. Nicola,¹⁰ D. Norman,⁴⁵
 L. Oesch,²⁴ V. Oguri,³⁸ E. Oltman,²² N. Oshima,¹⁴ D. Owen,²⁵ P. Padley,³⁷ M. Pang,¹⁹
 A. Para,¹⁴ C.H. Park,¹⁴ Y.M. Park,²¹ R. Partridge,⁵ N. Parua,⁴³ M. Paterno,³⁹ J. Perkins,⁴⁴
 A. Peryshkin,¹⁴ M. Peters,¹⁶ H. Piekarz,¹⁵ Y. Pischalnikov,³⁶ V.M. Podstavkov,³⁵ B.G. Pope,²⁵
 H.B. Prosper,¹⁵ S. Protopopescu,⁴ D. Pušeljčić,²² J. Qian,²⁴ P.Z. Quintas,¹⁴ R. Raja,¹⁴
 S. Rajagopalan,⁴² O. Ramirez,¹⁷ M.V.S. Rao,⁴³ P.A. Rapidis,¹⁴ L. Rasmussen,⁴² S. Reucroft,²⁹
 M. Rijssenbeek,⁴² T. Rockwell,²⁵ N.A. Roe,²² P. Rubinov,³¹ R. Ruchti,³² J. Rutherford,²
 A. Sánchez-Hernández,¹¹ A. Santoro,¹⁰ L. Sawyer,⁴⁴ R.D. Schamberger,⁴² H. Schellman,³¹
 J. Sculli,²⁸ E. Shabalina,²⁶ C. Shaffer,¹⁵ H.C. Shankar,⁴³ R.K. Shivpuri,¹³ M. Shupe,²
 J.B. Singh,³⁴ P.P. Singh,³⁰ V. Sirotenko,³⁰ W. Smart,¹⁴ A. Smith,² R.P. Smith,¹⁴ R. Snihur,³¹
 G.R. Snow,²⁷ J. Snow,³³ S. Snyder,⁴ J. Solomon,¹⁷ P.M. Sood,³⁴ M. Sosebee,⁴⁴ M. Souza,¹⁰
 A.L. Spadafora,²² R.W. Stephens,⁴⁴ M.L. Stevenson,²² D. Stewart,²⁴ D.A. Stoianova,³⁵
 D. Stoker,⁸ K. Streets,²⁸ M. Strovink,²² A. Sznajder,¹⁰ P. Tamburello,²³ J. Tarazi,⁸
 M. Tartaglia,¹⁴ T.L. Taylor,³¹ J. Thompson,²³ T.G. Trippe,²² P.M. Tuts,¹² N. Varelas,²⁵
 E.W. Varnes,²² P.R.G. Virador,²² D. Vititoe,² A.A. Volkov,³⁵ A.P. Vorobiev,³⁵ H.D. Wahl,¹⁵
 G. Wang,¹⁵ J. Warchol,³² G. Watts,⁵ M. Wayne,³² H. Weerts,²⁵ A. White,⁴⁴ J.T. White,⁴⁵
 J.A. Wightman,¹⁹ J. Wilcox,²⁹ S. Willis,³⁰ S.J. Wimpenny,⁹ J.V.D. Wirjawan,⁴⁵ J. Womersley,¹⁴
 E. Won,³⁹ D.R. Wood,²⁹ H. Xu,⁵ R. Yamada,¹⁴ P. Yamin,⁴ C. Yanagisawa,⁴² J. Yang,²⁸
 T. Yasuda,²⁹ P. Yepes,³⁷ C. Yoshikawa,¹⁶ S. Youssef,¹⁵ J. Yu,¹⁴ Y. Yu,⁴¹ Q. Zhu,²⁸ Z.H. Zhu,³⁹
 D. Zieminska,¹⁸ A. Zieminski,¹⁸ E.G. Zverev,²⁶ and A. Zylberstejn⁴⁰

¹ Universidad de los Andes, Bogotá, Colombia

² University of Arizona, Tucson, Arizona 85721

³ Boston University, Boston, Massachusetts 02215

⁴ Brookhaven National Laboratory, Upton, New York 11973

⁵ Brown University, Providence, Rhode Island 02912

⁶ Universidad de Buenos Aires, Buenos Aires, Argentina

⁷ University of California, Davis, California 95616

⁸ University of California, Irvine, California 92717

⁹ University of California, Riverside, California 92521

¹⁰ LAFEX, Centro Brasileiro de Pesquisas Físicas, Rio de Janeiro, Brazil

¹¹ CINVESTAV, Mexico City, Mexico

¹² Columbia University, New York, New York 10027

¹³ Delhi University, Delhi, India 110007

- ¹⁴Fermi National Accelerator Laboratory, Batavia, Illinois 60510
¹⁵Florida State University, Tallahassee, Florida 32306
¹⁶University of Hawaii, Honolulu, Hawaii 96822
¹⁷University of Illinois at Chicago, Chicago, Illinois 60607
¹⁸Indiana University, Bloomington, Indiana 47405
¹⁹Iowa State University, Ames, Iowa 50011
²⁰Korea University, Seoul, Korea
²¹Kyungshung University, Pusan, Korea
²²Lawrence Berkeley National Laboratory and University of California, Berkeley, California 94720
²³University of Maryland, College Park, Maryland 20742
²⁴University of Michigan, Ann Arbor, Michigan 48109
²⁵Michigan State University, East Lansing, Michigan 48824
²⁶Moscow State University, Moscow, Russia
²⁷University of Nebraska, Lincoln, Nebraska 68588
²⁸New York University, New York, New York 10003
²⁹Northeastern University, Boston, Massachusetts 02115
³⁰Northern Illinois University, DeKalb, Illinois 60115
³¹Northwestern University, Evanston, Illinois 60208
³²University of Notre Dame, Notre Dame, Indiana 46556
³³University of Oklahoma, Norman, Oklahoma 73019
³⁴University of Panjab, Chandigarh 16-00-14, India
³⁵Institute for High Energy Physics, 142-284 Protvino, Russia
³⁶Purdue University, West Lafayette, Indiana 47907
³⁷Rice University, Houston, Texas 77251
³⁸Universidade Estadual do Rio de Janeiro, Brazil
³⁹University of Rochester, Rochester, New York 14627
⁴⁰CEA, DAPNIA/Service de Physique des Particules, CE-SACLAY, France
⁴¹Seoul National University, Seoul, Korea
⁴²State University of New York, Stony Brook, New York 11794
⁴³Tata Institute of Fundamental Research, Colaba, Bombay 400005, India
⁴⁴University of Texas, Arlington, Texas 76019
⁴⁵Texas A&M University, College Station, Texas 77843

b' PHENOMENOLOGY

Standard sequential fourth generation quarks (b' , t') are pair-produced by the strong interaction with the same cross section, for a given mass, as the top quark (1-3). Standard Model weak decays of either quark can proceed via the charged current (CC) (Fig. 1(a)), or via loop-induced flavor changing currents (FCNC) (Fig. 1(b),(c)). Ordinarily, FCNC decay modes are far weaker than corresponding CC decay modes due to the former being higher order in the weak interaction, as well as due to possible suppression by GIM mechanism (4).

It was realized in the late 1980's that a sufficiently light b' quark (*i.e.* $m_{b'} < m_t$) offers a plausible scenario for the weak FCNC decay to be the dominant decay mechanism (5). If the b' quark is lighter than both the t and t' quark, then the CC decay to either is kinematically forbidden. In that case, the dominant CC decay mechanism of b' is to the charm quark, which is Cabibbo suppressed due to changing the generation number by two. In contrast, the FCNC decay of b' to the b quark is only required to change the generation number by one. The relative strength of b' CC and FCNC decay will depend on the details of the CKM matrix and the t , b' and t' quark masses.

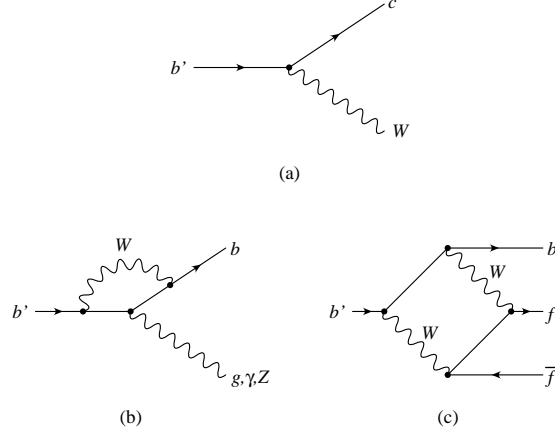


FIG. 1. Weak decays of the b' quark: (a) charged current, (b) electroweak penguin, (c) box diagram.

Direct Experimental Constraints on Fourth Generation Quarks

Fourth generation quarks of either charge that decay via the CC to bottom or charm quarks have experimental signatures that are very similar to top quark signatures that have been searched for by CDF and DØ. Except for polarization effects, the dilepton and untagged single lepton signatures are identical to top quark signatures. Only the b -tagged signature is not the same in the case of decay to the charm quark. The DØ mass limit of $m_t > 131 \text{ GeV}/c^2$ (6), which did not make use of b -tagging, will apply with little modification to the lighter of b' or t' on the assumption of predominant CC decay.

The FCNC scenario is less constrained by experiment. Direct searches for FCNC b' quark decay signatures were carried out at e^+e^- colliders soon after the prediction of a substantial FCNC decay of b' (7). Limits are also obtained from measurement of R and the Z width. The LEP I data have ruled out b' with masses up to $m_Z/2$ regardless of the decay mode (8). Until now, the $p\bar{p}$ collider experiments have not searched for or placed limits on b' quarks with substantial FCNC decay branching ratios.

Indirect Constraints on Fourth Generation Quarks

An indirect limit on the existence of fourth generation quarks comes from the ρ parameter ($\rho = m_W^2/(m_Z^2 \cos^2 \theta_W)$). In the Standard Model $\rho = 1$ at tree level. Radiative corrections generate a positive contribution to ρ from each non-degenerate weak isodoublet (9):

$$\Delta\rho = \frac{G_F C}{8\sqrt{2}\pi^2} \Delta m^2, \quad (1)$$

where C is a color factor (*i.e.* $C = 3$ for quarks), and

$$\Delta m^2 = m_1^2 + m_2^2 - \frac{4m_1^2 m_2^2}{m_1^2 - m_2^2} \ln \frac{m_1}{m_2} \quad (2)$$

$$\geq (m_1 - m_2)^2 \quad (3)$$

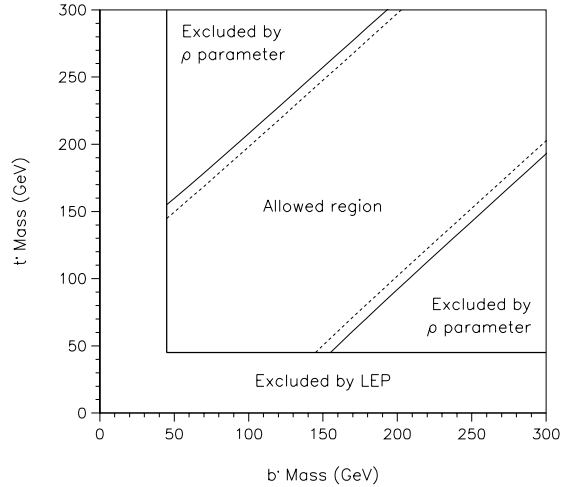


FIG. 2. Region of $m_{b'}-m_{t'}$ plane allowed by direct (thick line) and indirect experimental constraints at 95% CL (solid line) and 90% CL (dashed line).

is the mass splitting of the isodoublet. Assuming that the interpretation of the observed top quark signals by CDF and DØ is correct, most of the known deviation of ρ from unity is accounted for by the large m_b-m_t mass splitting. Any additional positive contributions to $\Delta\rho$ from fourth generation quarks and leptons, or other new particles, are limited according to the following equation (9):

$$m_t^2 + \sum_i \frac{C_i}{3} \Delta m_i^2 \leq (210 \text{ GeV})^2 \quad (95\% \text{ CL}). \quad (4)$$

In order to avoid a large discrepancy between the predicted and measured value of ρ , a light b' quark also implies a relatively light t' quark. The allowed region in the $m_{b'}-m_{t'}$ plane is shown in Fig. 2.

It has also been suggested that the t quark signatures observed by CDF and DØ are due to t' rather than t , and the third generation t quark itself has not been seen because it decays by an exotic (supersymmetry or Higgs) decay mode (10,11). In such cases, indirect limits on $m_{b'}$ are much weaker.

FCNC Decay Modes of the b'

The FCNC decay modes of the b' quark are generally to a b quark and a gauge boson or fermion pair:

TABLE 1. Calculated FCNC branching ratios of the b' quark for $m_{b'} = 80$ GeV.

Decay Mode	Branching Ratio (%)
$b' \rightarrow b\gamma$	12.6
$b' \rightarrow bg$	52.1
$b' \rightarrow be^+e^-$	1.3
$b' \rightarrow b\nu\bar{\nu}$	7.8
$b' \rightarrow bq\bar{q}$	26.2

$$\begin{aligned}
&b' \rightarrow b g \\
&b' \rightarrow b \gamma \\
&b' \rightarrow b Z^0 \\
&b' \rightarrow b \ell^+ \ell^- \\
&b' \rightarrow b q \bar{q} \\
&b' \rightarrow b H^0
\end{aligned}$$

The neutral Higgs boson decay mode is expected to be dominant if it is kinematically accessible. Otherwise, the Z boson decay mode is dominant for sufficiently heavy b' , dominating even the gluon mode. The present search made use of only those signatures involving at least one photon. Because of Z dominance, the sensitivity of the photon signatures are limited to b' masses not much above the Z mass. The branching ratios of the various FCNC decay modes are calculable in the Standard Model (12). Some calculated branching ratios are listed in Table 1.

PARTICLE DETECTION

The $D\phi$ detector and data collection systems are described in Ref. (13).

Muons are detected and momentum-analyzed using an iron toroid spectrometer located outside of a uranium-liquid argon calorimeter and a non-magnetic central tracking system inside the calorimeter. Muons are identified by their ability to penetrate the calorimeter and the spectrometer magnet yoke. The muons used for b -tagging are required to be within distance $\Delta\mathcal{R} < 0.5$ of any jet axis.

Photons are identified by their longitudinal and transverse shower profile in the calorimeter and by the absence of matching tracking chamber hits along a road between the calorimeter cluster and any reconstructed vertex.

Jets are reconstructed using a cone algorithm of radius $\mathcal{R} = 0.5$.

SIGNATURES

The $D\phi$ experiment has searched for b' pair production signatures in which at least one b' quark decays via the photon FCNC mode. The two final state signatures are $\gamma + 3$ jets and $2\gamma + 2$ jets depending on whether one or both b' quarks decay via the photon mode. In the case of the single photon signature, the second b' quark is assumed to decay via the gluon decay mode $b' \rightarrow bg$. A soft muon b tag is required in the case of the single photon signature.

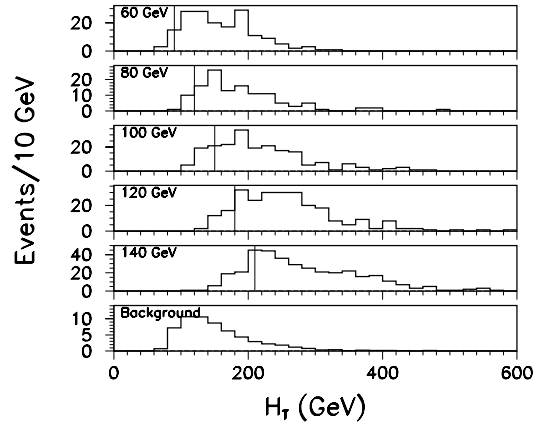


FIG. 3. Monte Carlo b' H_T distribution for the single photon analysis for several different b' masses.

Analysis of $b'\bar{b}' \rightarrow \gamma + 3 \text{ jets} + \mu\text{-tag}$

This signature occurs when one b' decays to a photon and the second b' decays to a gluon or otherwise hadronically. The two main backgrounds to this signature are high- p_T photon + jets production, and multijet production with a fake photon. Less important backgrounds are diboson ($W\gamma$ and $Z\gamma$) and single W and Z boson production with an electron identified as a photon.

This analysis sample has an integrated luminosity of 90 pb^{-1} .

Event Selection

The event selection cuts are as follows:

- One photon in the central cryostat ($|\eta| < 1.1$) with $E_T > 20 \text{ GeV}$.
- Three or more jets with $E_T > 15 \text{ GeV}$ and $|\eta| < 2$.
- At least one tagging muon with $|\eta| < 1.1$ and $p_T > 4 \text{ GeV}$.
- $H_T > 1.5m_{b'}$.

The quantity H_T used in the final cut is defined as the scalar sum of the E_T 's of the photon and the jets. Note that the H_T depends on the b' mass hypothesis. The value of the H_T cut given above is nearly optimal, in terms of maximizing sensitivity, for all of the b' masses considered. Figure 3 shows H_T distributions of Monte Carlo b' events. Figure 4 shows the significance, defined as acceptance divided by the square root of the background, as a function of the H_T cut for different b' masses.

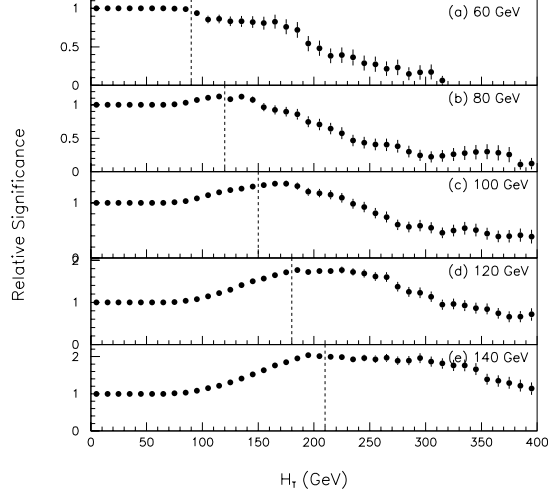


FIG. 4. Relative significance (A/\sqrt{B}) for the single photon analysis as a function of the H_T cut for several different b' masses.

TABLE 2. Acceptance for $b'b' \rightarrow \gamma + 3 \text{ jets} + \mu\text{-tag}$ for different b' masses.

$m_{b'}$ (GeV)	Acceptance(%)
50	0.308 ± 0.069
60	0.697 ± 0.138
70	1.160 ± 0.212
80	1.441 ± 0.272
90	1.780 ± 0.318
100	2.227 ± 0.385
120	3.031 ± 0.514
140	3.818 ± 0.640

Acceptance Calculation

The acceptance for the single photon decay mode was calculated using the ISAJET version 7.14 event generator where one b' quark was forced to decay to a photon, and the second b' quark was forced to decay to a gluon. Table 2 gives the acceptance for several b' masses.

Background Calculation

The backgrounds considered in the analysis of the single photon signature are as follows:

- QCD production of high- p_T direct photons plus multiple jets.
- QCD multijet production with one jet misidentified as a photon.
- Diboson ($W\gamma$, $Z\gamma$).
- W and Z with electron misidentified as a photon.

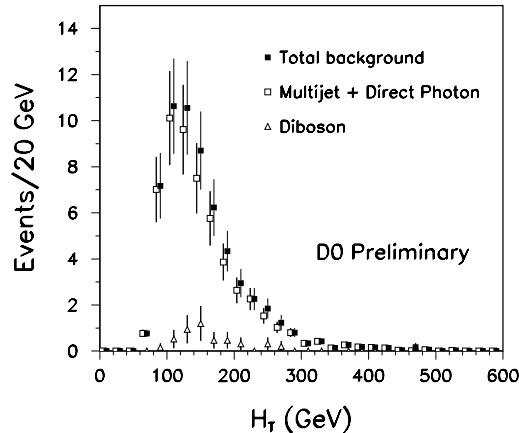


FIG. 5. H_T distributions for various backgrounds.

Major Backgrounds The first two of the above backgrounds are the main ones. These backgrounds are calculated by the tag rate method, which assumes that there is a universal per-jet background b -tagging rate for mixed flavor multijet processes. This is the same method that has been used to calculate the tagged W +jets backgrounds in the $D\bar{0}$ top quark analyses (14).

The tag rate function per jet is parameterized as a function of the following variables.

- Jet E_T .
- Jet η .
- Instantaneous luminosity.
- Time.

We assume that the tag rate function factorizes among the the above variables. We assume no non-trivial dependence on the number of jets, or in other words, that the tag rate per event is proportional to the number of jets.

Minor Backgrounds The diboson background ($Z\gamma$ and $W\gamma$) is expected to generate tags in excess of the background tag rate. These backgrounds have been estimated by a Monte Carlo calculation. The total estimated diboson background before the H_T cut is 4.6 ± 2.1 events, and is included in the background estimate.

The backgrounds from $W \rightarrow e + \text{jets}$ and $Z \rightarrow e + \text{jets}$ with the electron misidentified as a photon is estimated from the known electron-to-photon fake rate to be about 0.1 events. This background is neglected in the total background estimate.

Background Summary The H_T distributions of the various backgrounds are shown in Fig. 5. The total estimated background before the H_T cut is 59 ± 11 events with 71 events observed in the data. The H_T spectra of data and background are plotted in Fig. 6. There is a slight (not statistically significant) excess of data over background, which is mostly at low H_T .

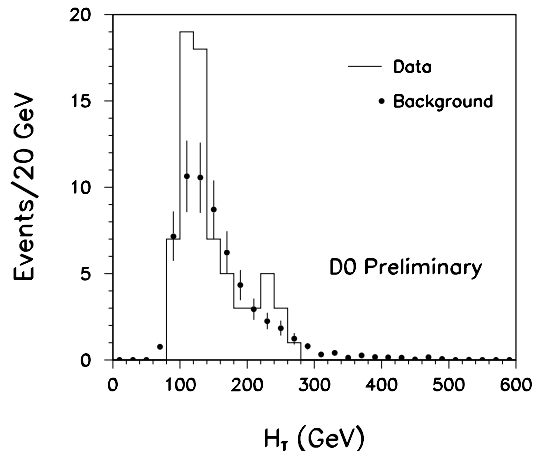


FIG. 6. H_T distributions of data and background in photon + three jet events.

Cross Section Calculation

Table 3 shows the number of observed events, the number of events expected for signal and background, and the calculated cross section times branching ratio as a function of b' mass. The number of expected events was calculated using the central theoretical cross section of Laenen *et al.* (1), and assuming the b' branching ratios of Table 1, namely $BR(b' \rightarrow b\gamma) = 13\%$ and $BR(b' \rightarrow bg) = 52\%$, giving a combined branching ratio of 13%. The cross section times branching ratio is calculated using the equation

$$\sigma_{b'\bar{b}'} \times BR = \frac{D - B}{A\mathcal{L}}, \quad (5)$$

where D is the number of data events, B is the expected background, A is the acceptance, and \mathcal{L} is the integrated luminosity. The error of the cross section times branching ratio is obtained by propagation of errors assuming Gaussian errors. The error of the integrated luminosity is set as 5.4%.

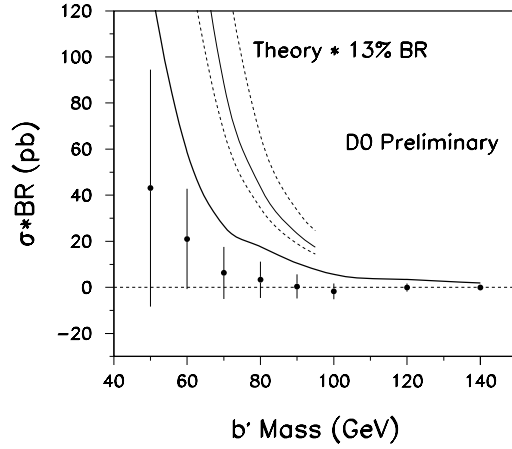
The measured value of $\sigma_{b'\bar{b}'} \times BR$ is the model independent result of the experiment. Further interpretation of this result can proceed by assuming a particular branching ratio and determining the cross section, as is done in the top quark search, or assuming the theoretical cross section and determining the branching ratio. The former type of interpretation is shown in Fig. 7, which compares the measured and theoretical cross section as a function of b' mass. The latter type of interpretation is shown in Fig. 8, which shows the measured branching ratio as a function of b' mass. In either case, the shown 95% CL upper limit curve is calculated excluding the unphysical negative cross section region of the likelihood.

Analysis of $b'\bar{b}' \rightarrow 2\gamma + 2$ jets

This signature occurs when both b' 's decay to photons. The main backgrounds are high- p_T photon + jets production with one fake photon, and multijet production with two fake

TABLE 3. The number of expected and observed photon + three jet events as a function of b' mass.

$m_{b'}$ (GeV/c ²)	Events			$\sigma_{b'\bar{b}'} \times BR$ (pb)	
	Observed	Expected Signal	Expected Background	Value	Upper limit (95% CL)
50	71	134 ± 31	59 ± 11	43.1 ± 51.4	133
60	69	126 ± 26	56 ± 11	21.0 ± 21.8	58.7
70	55	92 ± 18	49 ± 9	6.3 ± 11.3	26.7
80	45	56 ± 11	41 ± 8	3.3 ± 7.9	17.7
90	33	38 ± 7	32 ± 6	0.4 ± 5.2	10.5
100	22	27 ± 5	25 ± 5	-1.7 ± 3.4	5.6
120	15	14 ± 3	15 ± 3	-0.1 ± 1.8	3.4
140	9	8 ± 1	9 ± 2	-0.1 ± 1.0	1.9

**FIG. 7.** Comparison of measured cross section times branching ratio (points) and 95% CL upper limit (thick line) for $b'\bar{b}' \rightarrow \gamma + 3$ jets with the theoretical cross section of Laenen *et al.* (1) times an assumed branching ratio of 13%. The dashed theory curves are the author's upper and lower limit curve for the theoretical cross section.

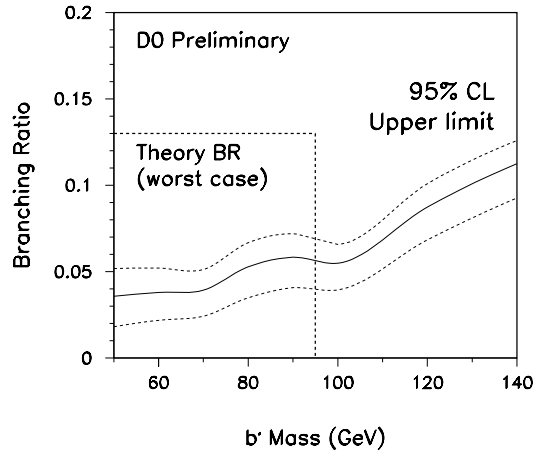


FIG. 8. Measured 95% CL upper limit on the branching ratio for $b'\bar{b}' \rightarrow \gamma + 3$ jets assuming the theoretical cross section of Laenen *et al.* (1). The dashed curves are obtained using the author's upper and lower theory curve, rather than the central theory curve.

photons. Minor backgrounds are from double direct photon production, and Drell-Yan and $Z \rightarrow ee$ with both electrons identified as photons.

This analysis has an integrated luminosity of 77 pb^{-1} .

Event Selection

The event selection cuts for this channel are as follows:

- Two photons with $E_T > 20 \text{ GeV}$ and $|\eta| < 2.0$.
- Two or more jets with $E_T > 15 \text{ GeV}$ and $|\eta| < 2.5$.
- $H_T > m_{b'} - 20 \text{ GeV}$.

For this analysis, H_T is defined as the scalar sum of the E_T 's of the jets, but not the photons. Figure 9 shows H_T distributions of Monte Carlo b' diphoton events. Figure 10 shows the significance, defined as acceptance divided by the square root of the background, as a function of the H_T cut for different b' masses.

Acceptance Calculation

The acceptance for the diphoton decay mode was calculated using the ISAJET event generator with both b' quarks forced to decay to a photon and a b quark. The calculated acceptances are shown in Table 4.

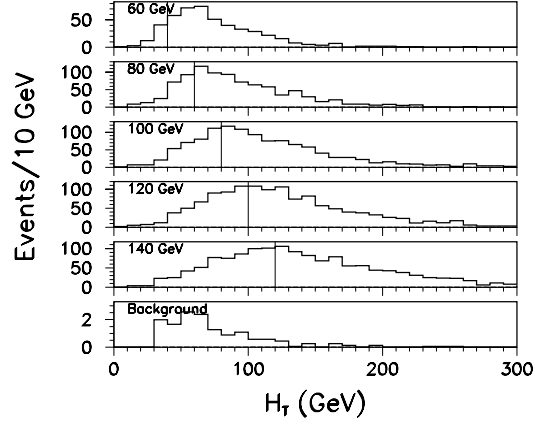


FIG. 9. Monte Carlo $b' H_T$ distributions for the diphoton analysis for several different b' masses.

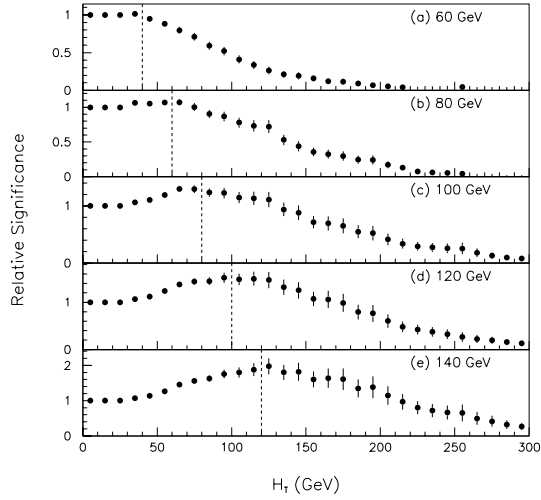


FIG. 10. Relative significance (A/\sqrt{B}) for the diphoton analysis as a function of the H_T cut for several different b' masses.

TABLE 4. Acceptance for $b'\bar{b}' \rightarrow 2\gamma + 2$ jets for different b' masses.

$m_{b'}$	Acceptance(%)
50	3.00 ± 0.38
60	5.34 ± 0.64
70	8.07 ± 0.92
80	10.15 ± 1.15
90	12.44 ± 1.38
100	13.37 ± 1.48
120	15.88 ± 1.74
140	17.74 ± 1.94

Background Calculation

The following backgrounds were considered:

- QCD high- p_T direct photon plus multijet events with one of the jets misidentified as a photon.
- QCD multijet production with two jets misidentified as photons.
- Double direct photon production.
- $Z \rightarrow ee$ plus jets events with both electrons misidentified as photons.

Major Backgrounds The first two backgrounds are the most important ones. The combination of the single and double fake backgrounds was estimated by the fake rate method. The fake background is the product of the number of events having a signature photon + electromagnetic cluster + two jets, times the electromagnetic cluster-to-photon fake rate. The fake rate used in this calculation is corrected for photon purity and combinatoric effects to account properly for the double fake background.

Minor Backgrounds The double direct photon background was estimated by a Monte Carlo calculation to be less than 0.05 events at 95% confidence. The double direct photon contribution to the background is neglected in the total background estimate.

The background from $Z \rightarrow ee +$ jets with both electrons faking photons is estimated from the known electron to photon fake rate to be 0.1 ± 0.1 events. This background was also neglected in the total background estimate.

Background Summary The total estimated single and double fake background before the H_T cut is 14.6 ± 2.2 events with 20 events observed in the data. The H_T distributions of data and background are shown in Fig. 11.

As a cross check, the entire event selection and background analysis was done with looser photon identification cuts. In this case, the expected background is 56.4 ± 3.1 events with 59 events observed in the data.

Cross Section Table 5 shows the number of observed events, the number of events expected for signal and background, and the calculated cross section times branching ratio as a function of b' mass. The number of expected events was calculated using the central theoretical cross section of Laenen *et al.* (1), and a branching ratio 1.6% for both b' quarks to decay to photons. Figure 12 shows the cross section times branching ratio, and the 95% CL upper limit, for various b' masses. Figure 13 shows the upper limit on the diphoton branching ratio, assuming the theoretical production cross section of Laenen *et al.*, as a function of b' mass.

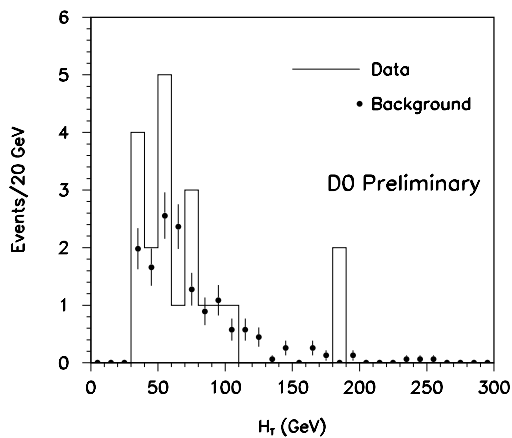


FIG. 11. H_T distributions of data and background in the diphoton mode.

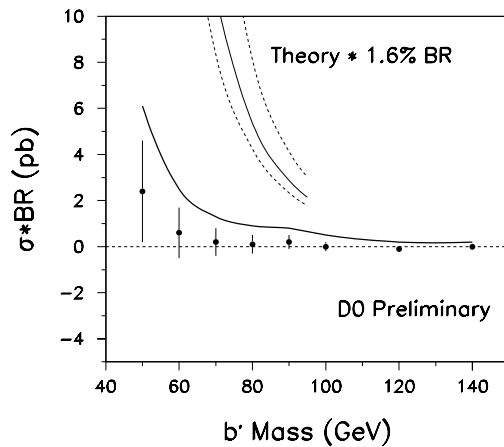


FIG. 12. Comparison of measured cross section times branching ratio (points) and 95% CL upper limit (thick line) for $b'\bar{b}' \rightarrow 2\gamma + 2 \text{ jets}$ with the theoretical cross section of Laenen *et al.* (1) times an assumed branching ratio of 1.6%. The dashed theory curves are the author's upper and lower limit curve for the theoretical cross section.

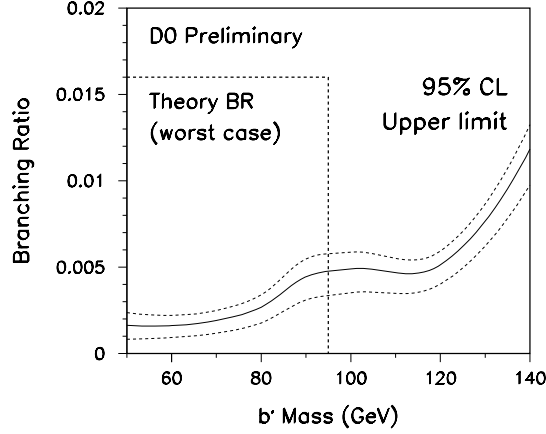


FIG. 13. Measured 95% CL upper limit on the branching ratio for $b'\bar{b}' \rightarrow 2\gamma + 2 \text{ jets}$ assuming the theoretical cross section of Laenen *et al.* (1). The dashed curves are obtained using the author's upper and lower theory curve, rather than the central theory curve.

TABLE 5. The number of expected and observed two photon + two jet events as a function of b' mass.

$m_{b'}$ (GeV/ c^2)	Events			$\sigma_{b'\bar{b}'} \times BR$ (pb)	
	Observed	Expected Signal	Expected Background	Value	Upper limit (95% CL)
50	20	137 ± 19	14.6 ± 2.2	2.4 ± 2.2	6.1
60	15	101 ± 13	12.6 ± 1.9	0.6 ± 1.1	2.5
70	12	67.2 ± 8.4	10.9 ± 1.7	0.2 ± 0.6	1.3
80	9	41.7 ± 5.2	8.4 ± 1.4	0.1 ± 0.4	0.9
90	8	27.4 ± 3.4	6.0 ± 1.0	0.2 ± 0.3	0.8
100	5	16.7 ± 2.1	4.7 ± 0.8	0.0 ± 0.2	0.5
120	2	7.6 ± 0.9	2.7 ± 0.6	-0.1 ± 0.1	0.2
140	2	3.7 ± 0.4	1.6 ± 0.4	0.0 ± 0.1	0.2

CONCLUSIONS

The $D\bar{D}$ experiment has searched for b' quark pair production via FCNC decay signatures where one or both b' quarks decays to a photon and a b quark. In both cases, we do not see a significant excess of events over the expected background. We set an upper limit on the cross section times branching ratio that is low enough to rule out b' quarks decaying predominantly via FCNC in the mass range $m_Z/2 < m_{b'} < m_Z + m_b$.

ACKNOWLEDGMENTS

We thank the staffs at Fermilab and the collaborating institutions for their contributions to the success of this work, and acknowledge support from the Department of Energy and National Science Foundation (U.S.A.), Commissariat à L'Energie Atomique (France), Ministries for Atomic Energy and Science and Technology Policy (Russia), CNPq (Brazil), Departments of Atomic Energy and Science and Education (India), Colciencias (Colombia), CONACyT (Mexico), Ministry of Education and KOSEF (Korea), CONICET and UBACyT (Argentina), and the A.P. Sloan Foundation.

REFERENCES

- * Visitor from IHEP, Beijing, China.
- † Visitor from Univ. San Francisco de Quito, Ecuador.
- 1. E. Laenen, J. Smith, and W. van Neerven, *Phys. Lett.* **321B**, 254 (1994).
- 2. E. Berger and H. Contopanagos, *Phys. Lett.* **361B**, 115 (1995).
- 3. S. Catani, M. L. Mangano, P. Nason, and L. Trentadue, CERN-TH-96-21, Jan. 1996.
- 4. S.L. Glashow, J. Iliopoulos, and L. Maiani, *Phys. Rev. D* **2**, 1285 (1970).
- 5. W.S. Hou, and R.G. Stuart, *Phys. Rev. Lett.* **62**, 617 (1989).
- 6. $D\bar{D}$ Collaboration, S. Abachi *et al.*, *Phys. Rev. Lett.* **72**, 2138 (1994).
- 7. VENUS Collaboration, K. Abe *et al.*, *Phys. Rev. Lett.* **63**, 1776 (1989);
AMY Collaboration, S. Eno *et al.*, *Phys. Rev. Lett.* **63**, 1910 (1989);
TOPAZ Collaboration, I. Adachi *et al.*, *Phys. Lett.* **234 B**, 197 (1990);
ALEPH Collaboration, D. Decamp *et al.*, *Phys. Lett.* **236B**, 511 (1990).
- 8. Particle Data Group, L. Montanet *et al.*, *Phys. Rev. D* **50**, 1442 (1995).
- 9. Particle Data Group, L. Montanet *et al.*, *Phys. Rev. D* **50**, 1312 (1995).
- 10. J.F. Gunion, D.W. McKay, and H. Pois, UCD-95-18, May 1995.
- 11. W.-S. Hou, *Phys. Rev. Lett.* **72**, 3945 (1994).
- 12. P. Agrawal, W.-S. Hou, *Phys. Rev. D* **46**, 1022 (1992).
- 13. $D\bar{D}$ Collaboration, S. Abachi *et al.*, *Nucl. Instrum. Methods* **A338**, 185 (1994).
- 14. $D\bar{D}$ Collaboration, S. Abachi *et al.*, "Top quark search with the $D\bar{D}$ 1992–1993 data sample," *Phys. Rev. D* **52**, 4877 (1995).